Cross sections of projectile-like fragments in the reaction $^{19}F + ^{66}Zn$ in the beam energy range of 3–6 MeV/nucleon

R. Tripathi,[1,*] K. Sudarshan,[1] S. Sodaye,[1] A. V. R. Reddy,[1] A. Goswami,[1] B. K. Nayak,[2] and S. K. Sharma[1]

[1]*Radiochemistry Division, Bhabha Atomic Research Centre, Mumbai, India*

[2]*Nuclear Physics Division, Bhabha Atomic Research Centre, Mumbai, India*

(Received 22 November 2008; revised manuscript received 4 February 2009; published 15 June 2009)

Angular distributions of projectile-like fragments (PLFs) have been measured in the reaction $^{19}F + ^{66}Zn$ at $E_{lab} = 61, 82, 92$, and 109 MeV to understand their formation in the low energy domain ($\lesssim$7 MeV nucleon). In this energy range, maximum angular momentum 'l_{max}' in the reaction is lower than or close to the critical or limiting angular momentum for complete fusion 'l_{lim}(CF).' The sum-rule model was modified to explain the cross sections of PLFs in the present study. For the first time, the modified sum-rule model, with a competition of incomplete fusion (ICF) reaction with complete fusion below l_{lim}(CF) reasonably reproduced the cross sections of PLFs in the beam energy range of the present study. It was observed that the cross sections of lighter PLFs fall more rapidly with decreasing beam energy compared to those of heavier PLFs, suggesting a change in the reaction mechanism from heavier to lighter PLFs. Transfer probabilities for peripheral collisions were calculated within the framework of a semiclassical formalism. The parameters of the nuclear potential required for the calculation of transfer probability were obtained by fitting the elastic scattering data measured in the present work. Calculated transfer probabilities were significantly lower compared to the corresponding experimental values, suggesting a significant overlap of the projectile and the target nuclei in incomplete fusion reactions. The present analysis showed that the overlap of the projectile and the target nuclei increases with increasing mass transfer at a given beam energy and for a given PLF, overlap increases with increasing beam energy.

DOI: 10.1103/PhysRevC.79.064604 PACS number(s): 25.70.Mn, 25.70.Hi

I. INTRODUCTION

Reactions involving incomplete mass transfer have been extensively studied in the past few decades. Such reactions may broadly be divided into three categories, namely, quasi-elastic transfer (QET) reactions, incomplete fusion (ICF) reactions, and deep inelastic collision (DIC). Quasi-elastic transfer reactions involve the transfer of only a few nucleons and are characterized by narrow kinetic energy spectra of projectile-like fragments (PLFs) peaking at optimum Q value (Q_{opt}) [1]. The contribution from ICF reaction leads to a low energy component in the kinetic energy spectra of PLFs [1–11]. Further, angular distribution of PLFs formed in ICF is forward peaked whereas those of PLFs formed in the QET reaction peak around the grazing angle [5]. In deep inelastic collision (DIC), the projectile and the target nuclei stick together for a sufficiently long time leading to a substantial dissipation of initial kinetic energy. Thus, in the case of DIC, the low energy tail in the kinetic energy spectra extends to the energy corresponding to the Coulomb repulsion in the exit channel. There is an exchange of nucleons between the colliding reaction partners in DIC, whereas ICF reactions involve the transfer of nucleons from a lighter to heavier reaction partner. Contributions from these reactions have been observed to vary depending on the projectile target combination and beam energy. At higher beam energies, typically ~10 MeV/nucleon or more, all of these mechanisms contribute to the formation of PLFs. At lower beam energies, QET and ICF mainly contribute to the formation of PLFs, particularly for the reaction systems with large entrance channel mass asymmetry.

Several models such as the sum-rule model [1,2], overlap model [12–15], break-up fusion model [16–18], and multistep direct reaction theory [19] were proposed to explain these reactions. Morgenstern *et al.* [20,21] correlated the probability of incomplete fusion reaction to the entrance channel mass asymmetry. However, none of these models could explain all the features of incomplete fusion reactions and it continues to be an active area of investigation [22–35]. Further, these models hold good only at higher beam energies. For example the sum-rule model successfully explained the cross section of PLFs in several reactions [1,2,36] at a beam energy of ~10 MeV/nucleon or more. However, it underestimates the cross section of PLFs at lower beam energies. According to this model, various transfer channels are localized in successive angular momentum windows beyond l_{crit} at which the pocket in the entrance channel potential for complete fusion vanishes. However, significant cross sections for the lighter PLFs, formed after large mass transfer, have been observed at lower beam energies which need to be explained. Brondi *et al.* modified the sum-rule model to explain the contribution from DIC along with ICF in the reaction $^{19}F + ^{56}Fe$ [4]. Measurement of cross sections of PLFs in the reaction $^{19}F + ^{89}Y$ as a function of beam energy showed that the cross sections of lighter PLFs decrease more rapidly with decreasing beam energy compared to those of heavier PLFs [35]. This observation was attributed to the requirement of significant overlap of the projectile and the target nuclei in reactions involving large mass transfer. Measurement of γ-ray multiplicity in coincidence with PLFs [37–39], and isomeric cross section ratio [40] also showed that the ICF reactions start

*Corresponding author: rahult@barc.gov.in

competing with the complete fusion at l-values lower than l_{crit}.

In order to understand the mechanism of formation of PLFs in an ICF reaction at lower beam energies, angular distributions of PLFs have been measured in the reaction $^{19}F + ^{66}Zn$ at $E_{lab} = 61, 82, 92,$ and 109 MeV. Angular distributions of PLFs were integrated to obtain their formation cross sections. Experimental cross sections of PLFs have been compared with those calculated using the sum-rule model [1,2]. Elastic scattering measurements were also carried out at similar beam energies. Elastic scattering data were used to calculate transfer probabilities for different transfer channels using a semiclassical formalism [41–45] which explains transfer reactions in terms of peripheral collisions. A variation in the transfer probability with beam energy for different channels, measured in the present study, has been compared with that observed in the reaction $^{19}F + ^{89}Y$ [35].

II. EXPERIMENTAL DETAILS

Experiments were carried out at BARC-TIFR Pelletron accelerator, Mumbai, India. A self-supporting target of enriched (>99%) ^{66}Zn of thickness 2 mg/cm^2 was mounted at the center of a scattering chamber of 1 m diameter. The target was bombarded with ^{19}F beam at energies of 65, 85, 95, and 112 MeV. Due to the degradation, average beam energies (E_{lab}) in the target were 61, 82, 92, and 109 MeV, respectively. Projectile-like fragments (PLFs) and scattered beam particles were detected using two silicon detector based E-ΔE particle identifier telescopes. The thickness of ΔE detectors was about 20 μm and that of E detectors was 1000 μm. Measurements were carried out in the angular range of 12°–65°. A monitor detector was kept at 15° to measure the elastically scattered beam particles. The data of the monitor detector were used to normalize the measured event rates in the telescopes for the beam current and target thickness to obtain absolute differential cross sections.

III. RESULTS AND DISCUSSION

The E-ΔE spectra of PLFs were transformed into particle identifier spectra. A typical particle identifier spectrum obtained in the reaction $^{19}F + ^{66}Zn$ at $E_{lab} = 109$ MeV ($\theta_{lab} = 24°$) is shown in Fig. 1. Spectra of different projectile-like fragments (PLFs) were projected on the energy axis to obtain their kinetic energy spectra. Kinetic energy spectra of PLFs at different angles were integrated to obtain their angular distributions in the laboratory frame of reference. Kinetic energy spectra of PLFs were transformed into the center of mass (c.m.) frame of reference to determine their kinetic energies in c.m. frame of reference. c.m. kinetic energies of PLFs were used to transform their laboratory angular distributions in the c.m. frame of reference. Angular distributions of PLFs ($Z_{PLF} = 3$–8) at $E_{lab} = 61, 82, 92,$ and 109 MeV are shown in Figs. 2(a)–2(d). Error bars on the data are due to counting statistics. Apart from the error due to the counting statistics, the systematic error on the differential cross sections is of the order of 10%, which is mainly due to the uncertainty in the

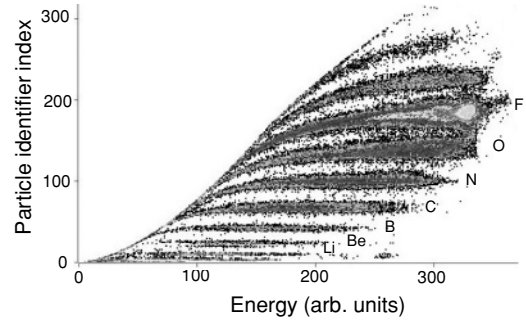

FIG. 1. A typical particle identifier spectrum in the reaction $^{19}F + ^{66}Zn$ ($E_{lab} = 109$ MeV; $\theta_{lab} = 24°$). Bands due to different PLFs are marked in this figure.

solid angles subtended by the monitor and telescope detectors. It can be seen from these figures that angular distributions of PLFs become more forward peaked with their decreasing proton number (Z_{PLF}). Angular distribution of PLFs such as O and N, having Z close to that of the projectile, tend to peak near the grazing angle, as observed usually for reactions involving the transfer a few nucleons at beam energies not much above the entrance channel Coulomb barrier. These observations indicate a progressive change in the reaction mechanism with increasing deviation of Z_{PLF} from that of the projectile. With an increase in beam energy, angular distributions of all the PLFs become forward peaked. Forward peaking of the angular distributions, ahead of the grazing angle, indicates a significant contribution from nuclear interaction in the formation of PLFs. This, in turn, indicates a large overlap of the projectile and the target nuclei in incomplete fusion reactions.

Plots of '$2\pi \sin\theta_{c.m.}\, d\sigma/d\Omega$' versus $\theta_{c.m.}$ were subjected to Gaussian fitting with weight of the error on the individual data points. In the fitting process, centroid, width, and area under the Gaussian curve were kept as free parameters. The fitted curves were integrated to obtain the cross sections of PLFs, which are shown as a function of beam energy in Fig. 3. The uncertainty quoted on the cross sections is due to the error on the fitted area. It can be seen from this figure that the cross sections of lighter PLFs decrease sharply compared to those of heavier PLFs with decreasing beam energy. This observation is consistent with that observed in our earlier study of the reaction $^{19}F + ^{89}Y$ [35]. The rapid fall in the cross section of lighter PLFs can be qualitatively explained by assuming that they are predominantly formed in the collision trajectories involving a large overlap of the projectile and the target nuclei. For a given impact parameter or degree of overlap between the projectile and the target nuclei, the angular momentum increases with increasing beam energy. Thus, collision trajectories involving a large overlap of the projectile and the target nuclei may lead to an incomplete fusion reaction at higher beam energies, which will otherwise lead to complete fusion at lower beam energies.

A. Sum-rule model calculations

Wilczynski *et al.* [1,2] developed the sum-rule model to explain the cross section for complete fusion and incomplete

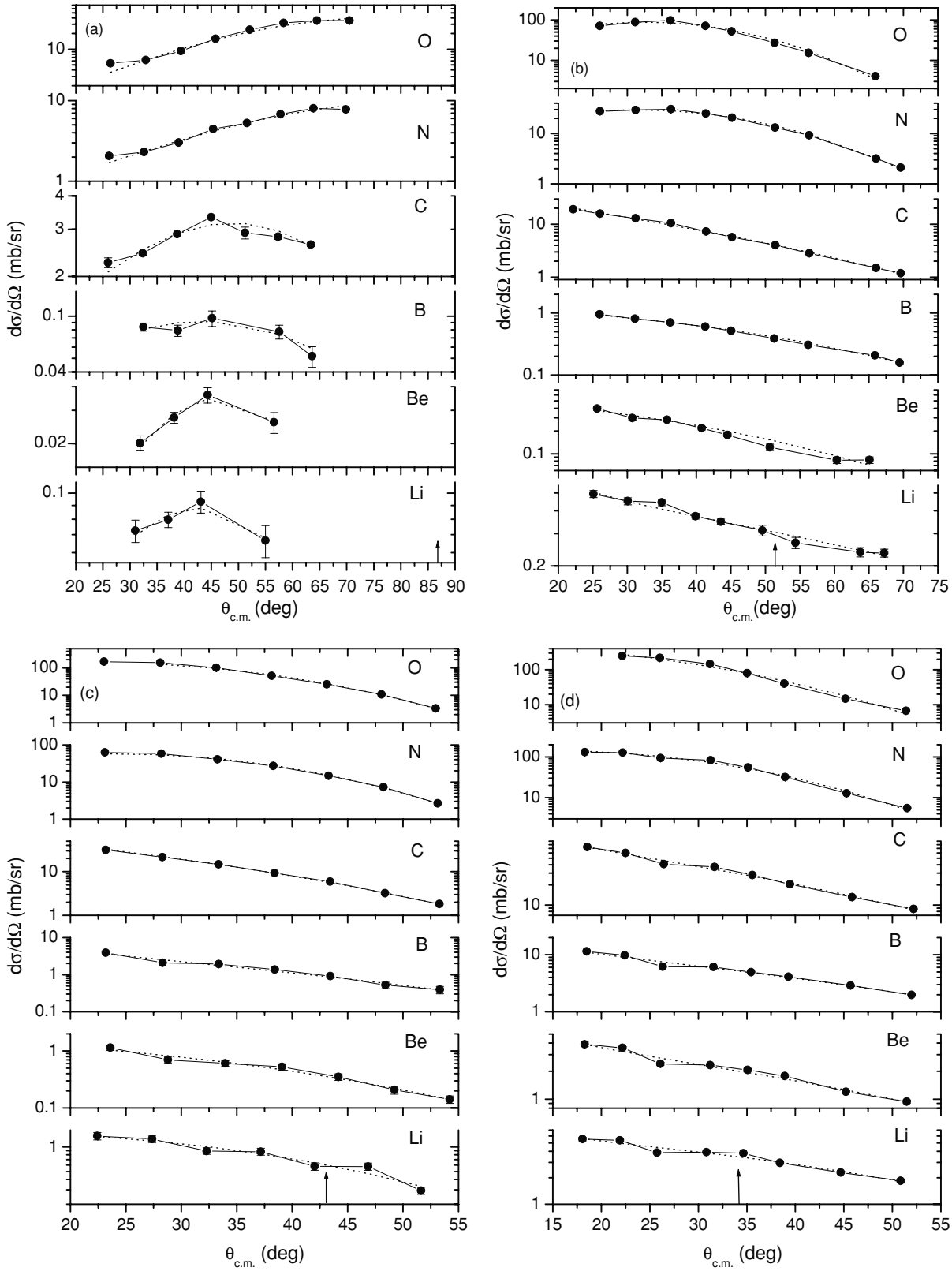

FIG. 2. Center of mass angular distributions of projectile-like fragments (PLFs) with $Z_{PLF} = 3$–8 in the reaction $^{19}F + ^{66}Zn$ at (a) $E_{lab} =$ 61 MeV, (b) $E_{lab} = 82$ MeV, (c) $E_{lab} = 92$ MeV, (d) $E_{lab} = 109$ MeV. Dotted lines are fitted curves. The arrow marks the grazing angle at the corresponding beam energy.

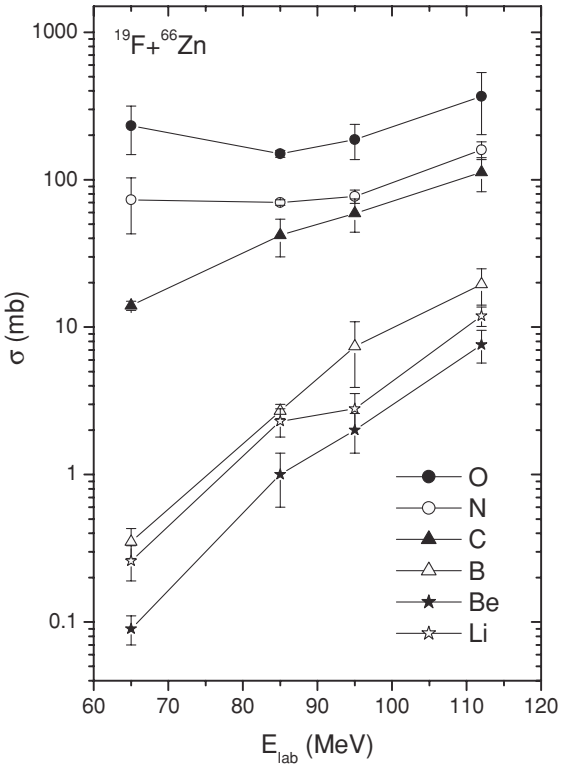

FIG. 3. Cross sections of projectile-like fragments (PLFs) with $Z_{PLF} = 3$–8 in the reaction $^{19}F + ^{66}Zn$ as a function of beam energy (E_{lab}).

fusion reactions. This model explains incomplete fusion reactions in terms of peripheral collisions. According to this model, the cross section for a particular reaction channel 'i' is given by the following equation:

$$\sigma(i) = \pi \lambda\!\!\!^{-2} \sum_{l=0}^{l_{max}} (2l+1) \frac{T_l(i)p(i)}{\sum_j T_l(j)p(j)}, \qquad (1)$$

where $\lambda\!\!\!^{-} = \hbar/\sqrt{2\,\mu E}$ is the reduced wavelength at beam energy E and μ is the reduced mass. $p(i)$ is the probability for the reaction channel 'i' and is proportional to $e^{[Q_{gg}(i)-Q_C(i)]/T}$, where $Q_{gg}(i)$ is the ground state Q value and $Q_C(i)$ is the change in Coulomb interaction energy due to the transfer of charge for the reaction channel 'i' [46]. The transmission coefficient $T_l(i)$ is given by the following equation [1]:

$$T_l(i) = \left[1 + \exp\left(\frac{l - l_{lim}(i)}{\Delta}\right)\right]^{-1}, \qquad (2)$$

where $l_{lim}(i)$ is equal to '$(A_P/n)l_{crit}(i)$,' $l_{crit}(i)$ is the critical angular momentum at which the pocket in the entrance channel potential vanishes for the reaction channel 'i' [47], Ap is the projectile mass number, and 'n' is the number of transferred nucleons. The parameter 'Δ' is the diffuseness of the l-distribution. Sum-rule model calculations involve three parameters, namely, effective temperature T, critical distance R_c, and diffuseness parameter Δ [1]. Wilczynski *et al.* [1] obtained $T = 3.5$ MeV, $R_c = 1.5(A_P^{1/3} + A_T^{1/3})$, and $\Delta = 1.7\hbar$ from the best fit to the experimental cross sections of PLFs in the reaction $^{14}N + ^{159}Tb$ at $E_{lab} =$ 140 MeV. In the present calculations, R_c and Δ values have been taken the same as used by Wilczynski *et al.* [1]. The value of the effective temperature (T) was varied to minimize the chi-square between the calculated and the experimental values. In the calculation of chi-square, the yield of 'Be' was excluded as its experimental yield was underestimated due to the break up of ^{8}Be into two α particles. Calculated and experimental cross sections of PLFs ($Z_{PLF} = 3$–8) are shown in Fig. 4. Effective temperature (T) values corresponding to the minimum chi-square are also shown in the figure. It can be seen from this figure that the sum-rule calculations grossly underestimate the cross sections of PLFs, particularly at the lower three beam energies. Underestimation of the cross section of PLFs by the sum-rule model is related to the localization of different reaction channels in the angular momentum space which is decided by quantities '$p(i)$' and

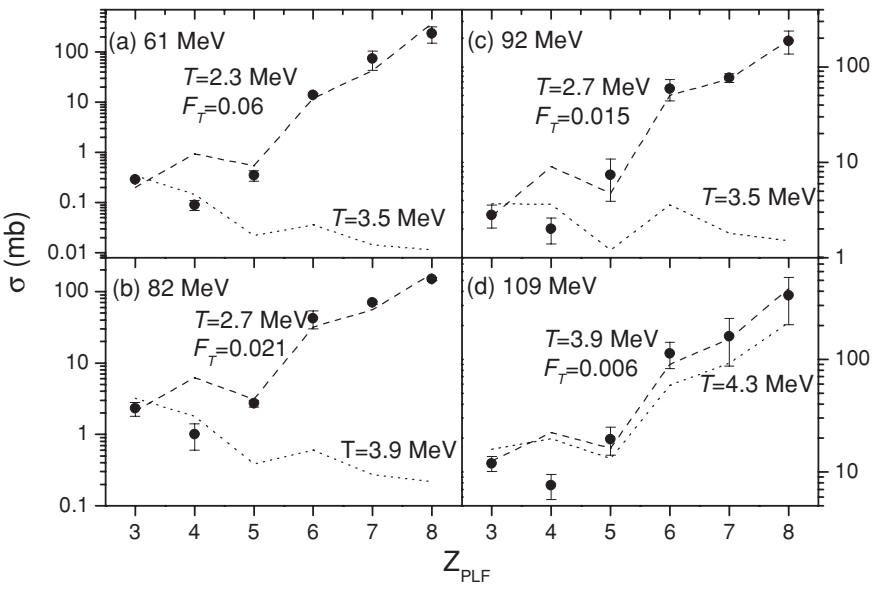

FIG. 4. Comparison of calculated and experimental cross sections of projectile-like fragments in the reaction $^{19}F + ^{66}Zn$ at $E_{lab} = 61$, 82, 92, and 109 MeV. Dotted lines are sum-rule model [1,2] calculations. Temperature (T) values corresponding to minimum chi-square are given along with the dotted lines. Dashed lines are modified sum-rule model calculations. The values of the temperature (T) and the parameter F_T corresponding to minimum chi-square are also given along with the dashed lines.

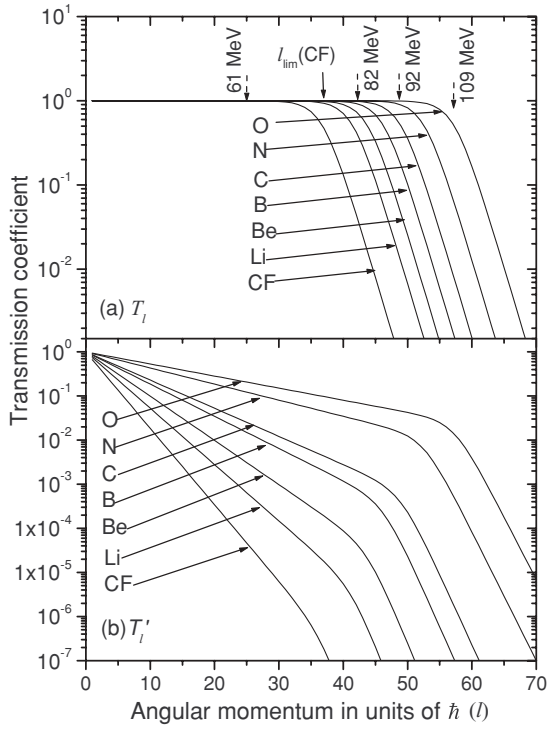

FIG. 5. Calculated transmission coefficients for transfer and complete fusion (CF) channels for the reaction $^{19}F + ^{66}Zn$. (a) Transmission coefficients (T_l) calculated according to sum-rule model (b) transmission coefficients (T_l') calculated for $E_{lab} = 82$ MeV using the modified sum-rule model. The solid arrow marks the limiting angular momentum for complete fusion 'l_{lim}(CF)' and dashed arrows mark the maximum angular momentum 'l_{max}' corresponding to different beam energies. Projectile-like fragments (PLFs) corresponding to different transfer channels are also shown in the figures.

'$T_l(i)$' in Eq. (1). A plot of calculated T_l values for complete fusion and other transfer channels in the reaction $^{19}F + ^{66}Zn$ is shown in Fig. 5(a). The limiting angular momentum for complete fusion l_{lim}(CF) and maximum angular momentum corresponding to different beam energies are marked in this figure. It can be seen from this figure that T_l values are close to unity for all the reaction channels at lower l values. However, due to the large value of $p(i)$ for complete fusion, the cross section for incomplete fusion becomes significant only for the l-values, for which, the T_l values for complete fusion become negligibly small. In order to illustrate the effect of $p(i)$, the overall probability for different reaction channels '$T_l(i)p(i)/\sum_j T_l(j)p(j)$,' was calculated using the sum-rule model with $T = 3.5$ MeV, $R_c = 1.5(A_P^{1/3} + A_T^{1/3})$, and $\Delta = 1.7\hbar$ [1,2]. Calculated reaction probabilities are shown as a function of l after multiplication with '$2l + 1$' in Fig. 6. Complete fusion (CF) and PLFs corresponding to different transfer channels are marked in this figure. Cross sections of N and C have been multiplied by a factor of 3 and those of B, Be, and Li have been multiplied by a factor of 10 for the clarity of the figure. Maximum angular momentum 'l_{max}' corresponding to different beam energies, and limiting angular momentum for complete fusion 'l_{lim}(CF)' are also marked in this figure. It can be seen from this figure that the complete fusion channel extends beyond l_{lim}(CF) due the large value of $p(i)$ for complete fusion. A similar result was obtained by Wilczynski *et al.* [1] in their calculation for the reaction $^{14}N + ^{159}Tb$. Further, it can be seen from this figure that there is no substantial cross section for PLFs, particularly for heavier PLFs, below the l_{max} value corresponding to $E_{lab} = 92$ MeV. Therefore, sum-rule model cross sections for these PLFs are not significant up to $E_{lab} = 92$ MeV. At $E_{lab} = 109$ MeV, l_{max} is sufficiently high so that cross sections for heavier PLFs are significantly increased. An increase in effective temperature T reduces the effect of $p(i)$ and brings sum-rule cross sections further close to the experimental values at $E_{lab} = 109$ MeV. However, at lower beam energies, an increase in T is not sufficient to explain the experimental cross sections of PLFs, as different transfer channels are localized beyond l_{max} of the reaction.

Observation of significant cross section for incomplete fusion at lower beam energies suggests that the incomplete fusion competes with complete fusion for collision trajectories

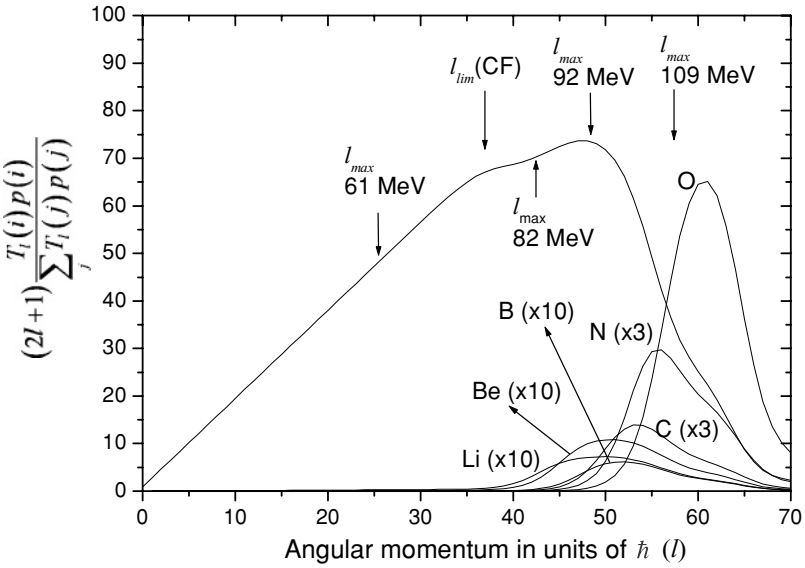

FIG. 6. Probability for complete fusion and different transfer channels as a function of angular momentum for the reaction $^{19}F + ^{66}Zn$, calculated using the sum-rule model [1,2] with $R = 1.5(A_P^{1/3} + A_T^{1/3})$, $\Delta = 1.7\hbar$, and $T = 3.5$ MeV. Limiting angular momentum for complete fusion l_{lim}(CF) and l_{max} corresponding to different beam energies are marked in the figure. Cross sections of N and C have been multiplied by a factor of 3 and those of B, Be, and Li are multiplied by a factor of 10 for clarity of the figure.

with $l < l_{\rm lim}$(CF). To account for this effect, Eq. (2) has been modified to the following:

$$T_l'(i) = \left[1 + \exp\left(\frac{l - l_{\rm lim}(i)}{\Delta}\right)\right]^{-1} (e^{nlF_T})^{-1}, \qquad (3)$$

where n is the number of transferred nucleons and F_T is a variable parameter which was obtained by minimizing the chi-square between the calculated and experimental cross sections of PLFs. The dependence of T_l' on the number of transferred nucleons 'n' is decided by the parameter F_T. With an increase in the F_T value, the decrease in T_l' with increasing 'n' becomes steeper. This results in a more rapid increase in the cross section of PLFs with their increasing mass (or Z). The cross sections of PLFs calculated using the modified T_l' values are shown in Fig. 4 as dashed lines. The parameter F_T and effective temperature T were varied to get the best agreement between the calculated and experimental values as judged by the chi-square. The values of F_T and T are also shown in the figure. It can be seen from this figure that the T values obtained in modified sum-rule model calculations are lower compared to those obtained in sum-rule model calculations. As modified sum-rule model calculations allowed contribution from lower l values to incomplete fusion, experimental cross sections of PLFs were reasonably reproduced with comparatively lower T values. The T values obtained in the modified sum-rule model calculations vary more systematically with beam energy compared to those obtained in sum-rule model calculations.

A typical plot of T_l' values, calculated for $E_{\rm lab} = 82$ MeV, is shown in Fig. 5(b). Due to the term $(e^{nlF_T})^{-1}$, the transmission coefficients for different transfer channels decrease with increasing l. Further, the decrease in the transmission coefficient becomes more rapid with increasing number of the transferred nucleons. Thus, the net effect of the incorporation of factor $(e^{nlF_T})^{-1}$ is to provide a competition from incomplete fusion reaction below $l_{\rm lim}$(CF), which is otherwise absent in the sum-rule model. F_T values obtained at different beam energies are plotted in Fig. 7. The rapid fall in the cross section of lighter PLFs results in an increase in F_T value with decreasing beam energy. The present calculations suggest that the significant cross section for incomplete fusion reaction at lower beam energies can be explained by considering the contribution from the collision trajectories with $l < l_{\rm lim}$(CF).

B. Transfer probability from a semiclassical formalism

In order to obtain an approximate estimate of the degree of overlap of the projectile and the target nuclei in incomplete fusion reactions, transfer probabilities for different channels were deduced from the c.m. angular distributions of PLFs using a semiclassical formalism [41,42] which explains the transfer reactions in terms of peripheral collisions. Differential cross sections of PLFs and corresponding center of mass angles ($\theta_{\rm c.m.}$) were transformed into 'transfer probability ($P_{\rm tr}$)' and 'distance of closest approach (D),' respectively, using the equations from Ref. [43]. Plots of '$P_{\rm tr}/\sin(\theta_{\rm c.m.}/2)$' versus the distance of closest approach 'D' for different transfer channels are shown in Fig. 8. It can be seen from this figure that the transfer channels involving the emission of O and N are localized in the D space. At lower D values, transfer probability falls as the overlap of the projectile and the target nuclei leads to complete fusion, whereas at higher D values, transfer probability for a given PLF falls because the overlap of the projectile and the target nuclei is insufficient for the

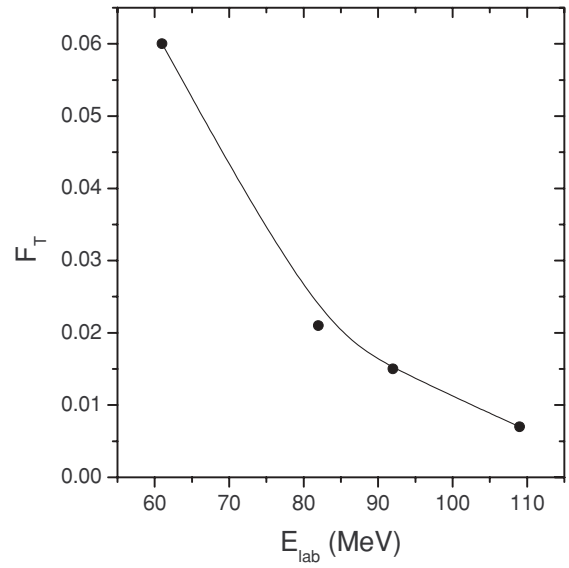

FIG. 7. Plot of F_T values obtained in modified sum-rule model calculations as a function of beam energy. The solid line is to guide the eye.

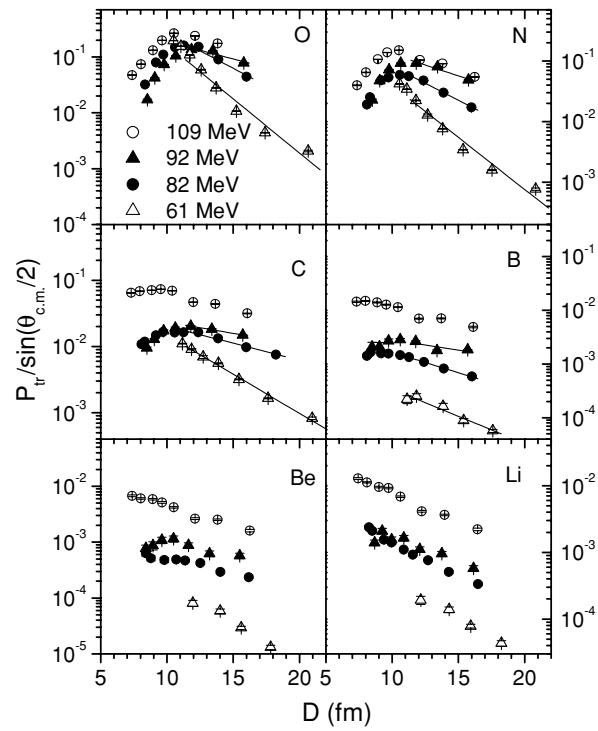

FIG. 8. Plot of transfer probability '$P_{\rm tr}/\sin(\theta_{\rm c.m.}/2)$' as a function of distance of closest approach (D) for transfer channels involving emission of projectile-like fragments (PLFs) with $Z_{\rm PLF} = 3$–8 in the reaction ^{19}F + ^{66}Zn at $E_{\rm lab} = 61, 82, 92$, and 109 MeV. Solid lines are the linear fit to the data.

formation of that PLF. For lighter PLFs C and B, such a localization is not seen at $E_{\rm lab} = 109$ MeV. Further, for Be and Li such localization is absent at all the beam energies of the present study. This observation suggests that, in the formation of these PLFs, the dinuclear system survives for a sufficiently long time to rotate before separation. This results in a weakening of the correlation between the transfer probability $P_{\rm tr}$ and emission angle $\theta_{\rm c.m.}$. In the present analysis, transfer probabilities have been calculated for PLFs with $Z_{\rm PLF} = 5$–8 for comparison with the experimental values at $E_{\rm lab} = 61$, 82, and 92 MeV.

According to the semiclassical formalism [41,42], transfer probability corresponding to the distance of closest approach 'D' is given by the following equation:

$$\frac{P_{\rm tr}(D)}{\sin(\theta_{\rm c.m.}/2)} = P_{\rm tr}(D_0)e^{-2\alpha(D-D_0)}, \tag{4}$$

where $P_{\rm tr}(D_0)$ is a normalization constant [41,42]. D_0 was taken as $1.65(A_p^{1/3} + A_T^{1/3})$ [45], where A_P and A_T are the mass numbers of the projectile and the target, respectively. In order to calculate the transfer probability, slope parameter 'α' was calculated using the expressions given in Refs. [43,48,49]. In present studies, masses of PLFs of a given Z were not resolved, therefore, α values for three transfer channels with positive or least negative Q_{gg} values were calculated. Calculated α values are given in Table I. Experimental α values, obtained by fitting the transfer probabilities at $D > D_0$ using Eq. (4), are also given in the table for comparison. It can be seen from this table that the experimental values are much lower compared to the calculated values.

In the studies by Nayak *et al.* [43], Biswas *et al.* [44], and Sahu *et al.* [45], it was shown that it is necessary to consider the contribution from nuclear interaction to explain the experimental transfer probabilities in quasi-elastic transfer reactions. Thus, the transfer probability ($P_{\rm tr}$) is given by the following equation:

$$P_{\rm tr}(D) = P_{\rm tr}(D_n)\frac{\sigma_{QE}(D_n)}{\sigma_T} + P_{\rm tr}(D_c)\frac{\sigma_{QE}(D_c)}{\sigma_T}, \tag{5}$$

where $P_{\rm tr}(D_n)\sigma_{QE}(D_n)$ and $P_{\rm tr}(D_C)\sigma_{QE}(D_c)$ represent the transfer cross sections for the nuclear and Coulomb branches of the classical deflection function and σ_T is the total cross section [$\sigma_T = \sigma_{QE}(D_n) + \sigma_{QE}(D_c)$]. D_c and D_n are the distances of closest approach corresponding to a c.m. angle $\theta_{\rm c.m.}$, which were obtained from the deflection function. The deflection functions for the interaction of ^{19}F with ^{66}Zn were calculated as a function of impact parameter 'b' using the following equation:

$$\Theta(b, E) = \pi - 2b\int_{r_{\rm min}}^{+\infty} dr\frac{1}{r^2}\left[1 - \frac{U_{\rm eff}(b, r)}{E}\right]^{-1/2}, \tag{6}$$

where $U_{\rm eff}(b, r)$ is the interaction potential between the colliding nuclei and is given as

$$U_{\rm eff}(b, r) = V_c(r) + V_n(r) + \frac{b^2E}{r^2}, \tag{7}$$

The first term in Eq. (7) is the Coulomb potential which is given by

$$V_c(r) = \frac{Z_PZ_Te^2}{2R_c}\left(3 - \frac{r^2}{R_c^2}\right); \quad r \leqslant R_c,$$
$$= \frac{Z_PZ_Te^2}{r}; \quad r > R_c, \tag{8}$$

where $R_c[= 1.2(A_P^{1/3} + A_T^{1/3})]$ is the sum of the radii of the projectile and the target nuclei. The value of R_c used in these calculations is different from that used in sum-rule model calculations. The value of the second term $V_n(r)$ is the real part of the nuclear potential, which was obtained by fitting the elastic scattering data of ^{19}F + ^{66}Zn at $E_{\rm lab} = 61$, 82, and 92 MeV using the optical model code SNOOPY 8Q [50],

TABLE I. Calculated and experimental α values for transfer channels corresponding to the emission of PLFs with $Z_{\rm PLF} = 5$–8 in the reaction ^{19}F + ^{66}Zn at $E_{\rm lab} = 61$, 82, and 92 MeV. For a given $Z_{\rm PLF}$, calculated values are given for the three transfer channels with positive or least negative Q_{gg} values. Uncertainty quoted on the experimental α values is due to the fitting error.

$Z_{\rm PLF}$	Ejectile	Q_{gg} (MeV)	$\alpha_{\rm calculated}$ (fm^{-1})	$\alpha_{\rm experimental}$ (fm^{-1})		
				61 MeV	82 MeV	92 MeV
8	^{18}O	−2.73	0.60	0.45 ± 0.05	0.29 ± 0.04	0.15 ± 0.05
	^{17}O	−2.49	1.10			
	^{16}O	3.68	1.37			
7	^{15}N	0.08	1.00	0.40 ± 0.03	0.26 ± 0.02	0.16 ± 0.04
	^{14}N	−3.34	1.78			
	^{13}N	−3.15	2.38			
6	^{14}C	−5.51	1.79	0.27 ± 0.01	0.12 ± 0.01	0.08 ± 0.01
	^{13}C	−5.28	2.07			
	^{12}C	0.57	2.23			
5	^{11}B	−6.84	2.05	0.23 ± 0.03	0.18 ± 0.01	0.09 ± 0.07
	^{10}B	−10.27	2.64			
	^{9}B	−7.55	2.86			

TABLE II. Parameters of optical model potential obtained by fitting elastic scattering data for $^{19}F + ^{66}Zn$ at $E_{lab} = 61, 82$, and 92 MeV using the code SNOOPY 8Q [50].

E_{lab} (MeV)	V_0 (MeV)	R_0 (fm)	a_0 (fm)	W (MeV)	$R_{i,0}$ (fm)	$a_{i,0}$ (fm)	σ_{Total} (mb)
61	40.10	1.08	0.559	24.45	1.21	0.449	1085
82	45.13	1.07	0.679	24.01	1.24	0.492	2415
92	41.77	1.09	0.787	27.40	1.18	0.665	3102

assuming the nuclear potential to be of Woods-Saxon form. Elastic scattering data along with the fitted curves are shown in Fig. 9. The parameters of the optical model potential obtained from the fitting are given in Table II. Total reaction cross sections are also given in this table. The last term in Eq. (7) is the centrifugal potential. The deflection function was obtained by integrating Eq. (6) after evaluating the Coulomb, nuclear, and centrifugal potentials. The lower limit of the integral in Eq. (6), r_{min}, outermost turning point of the collision trajectory, was obtained by solving the following equation:

$$V_c(r) + V_n(r) + \frac{b^2 E}{r_{min}^2} = 0. \quad (9)$$

Thus, Eq. (9) gives one to one correspondence between impact parameter 'b' and r_{min} or the distance of closest approach. The result of such a trajectory calculation for $E_{lab} = 82$ MeV is shown in Fig. 10. D_n and D_c values corresponding to a given

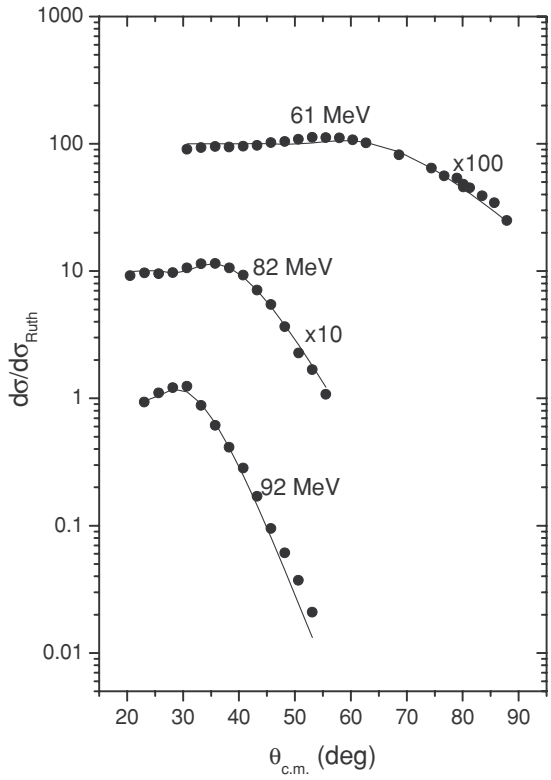

FIG. 9. Elastic scattering data along with the fitted curves for $^{19}F + ^{66}Zn$ at $E_{lab} = 61, 82$, and 92 MeV. Fitting was done using optical model code SNOOPY 8Q [50].

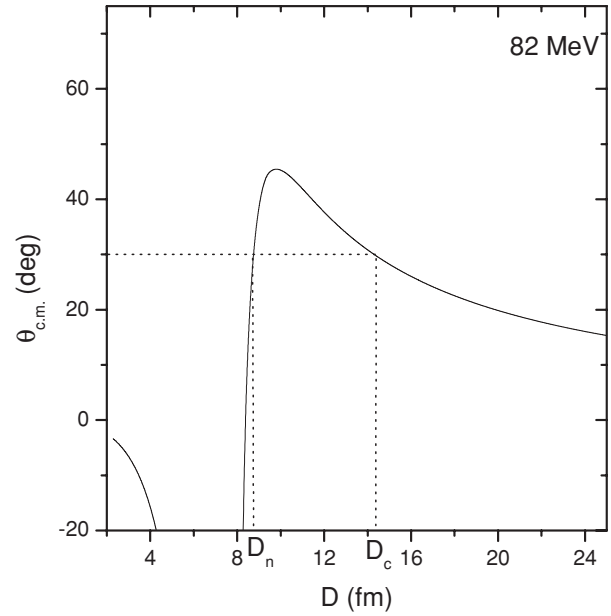

FIG. 10. Deflection function for $^{19}F + ^{66}Zn$ at $E_{lab} = 82$ MeV. D_n and D_c values corresponding to a single $\theta_{c.m.}$ are also shown in the figure.

c.m. angle are also shown in this figure. The cross sections $\sigma_{QE}(D_n)$ and $\sigma_{QE}(D_c)$ were calculated using the following equation:

$$\sigma(b) = \frac{b}{\sin(\theta)} \left| \frac{db}{d\theta} \right|. \quad (10)$$

$P_{tr}(D_n)$ and $P_{tr}(D_c)$ were calculated using Eq. (4). As the calculated α values were much higher compared to the experimental values, the lowest α value was taken for a given transfer channel while calculating $P_{tr}(D_n)$ and $P_{tr}(D_c)$. For $D < D_0$, $P_{tr}(D)$ was taken as $P_{tr}(D_0)$. As several l-waves are involved in the incomplete fusion reaction leading to the transfer of nucleons predominantly to the continuum states, angular distributions of PLFs do not show any oscillations. Therefore, $P_{tr}(D_n)$ and $P_{tr}(D_c)$ were added incoherently to obtain $P_{tr}(D)$, ignoring any effect due to the interference of Coulomb and nuclear trajectories.

Calculated values of $P_{tr}/\sin(\theta_{c.m.}/2)$ for PLFs with $Z_{PLF} =$ 5–8 are compared with the experimental values for $D > D_0$ in Fig. 11. Contributions from Coulomb and nuclear branches are shown as dashed and dotted lines, respectively. Solid lines represent the total transfer probability. The dotted line (nuclear contribution) merges with the solid line, when the contribution from Coulomb branch is small. It can be seen from this figure that the calculated nuclear contribution in a given transfer channel increases with increasing beam energy. However, even after including the nuclear contribution, the calculated transfer probabilities fall more rapidly with increasing 'D' compared to the experimental values. The comparatively slow decrease in experimental values with increasing 'D' is a manifestation of larger yields of PLFs at forward angle compared to that expected for peripheral collision, even after considering nuclear contribution. This observation suggests larger nuclear contribution in incomplete fusion reactions

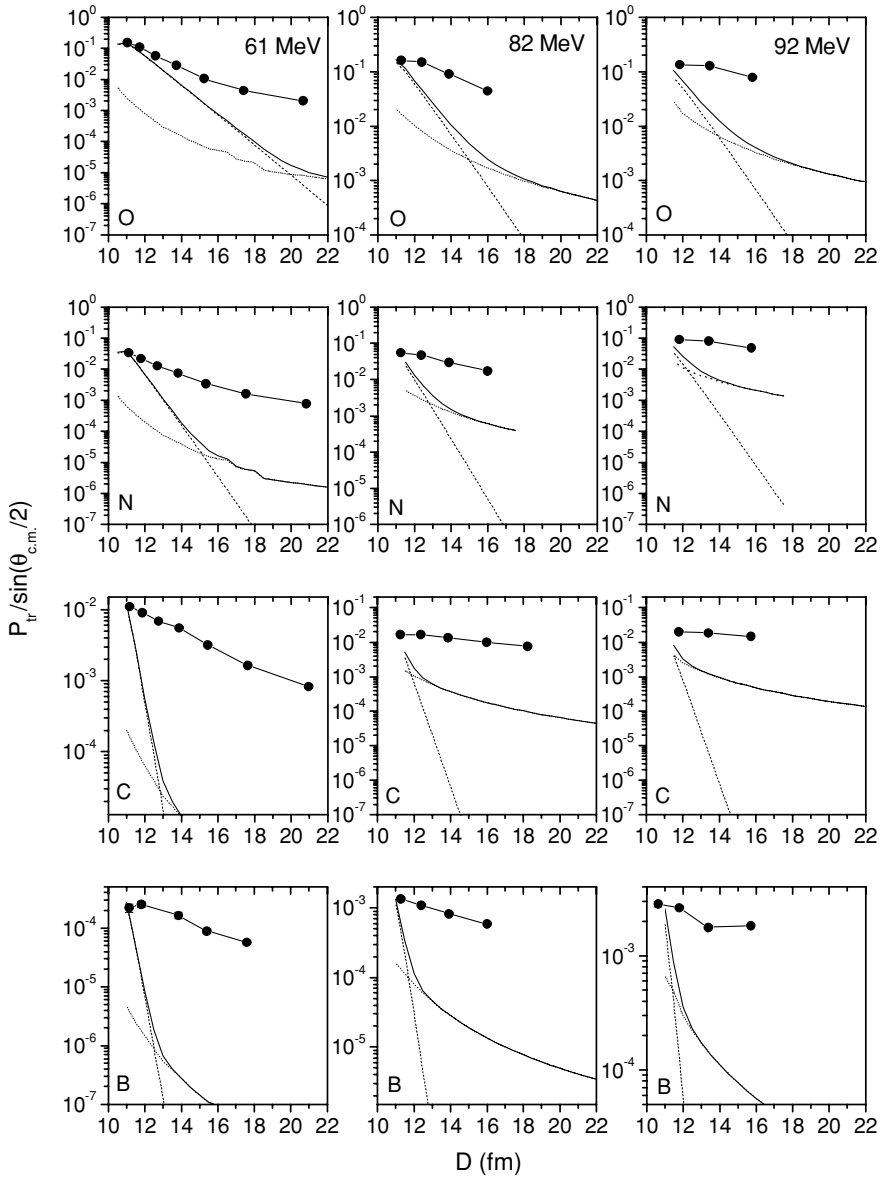

FIG. 11. Plot of transfer probability '$P_{\rm tr}/\sin(\theta_{\rm c.m.}/2)$' for transfer channels involving the emission of projectile-like fragments (PLFs) with $Z_{\rm PLF} = 5$–8 as a function of distance of closest approach (D) for $D > D_0$ {$=1.65(A_P^{1/3} + A_T^{1/3})$}; A_P and A_T are projectile and target mass numbers, respectively. '—●—' represents the experimental data. Dashed and dotted lines are, respectively, the calculated transfer contributions from Coulomb and nuclear branches of the classical deflection function. The solid line represents the total transfer probability. Dotted lines are merged with the solid lines when the contribution from Coulomb branch is small.

compared to that expected in peripheral collisions. Further, it can be seen that the discrepancy between the calculated and the experimental values increases with the increase in the number of transferred nucleons suggesting an increase in nuclear contribution. This observation suggests that the formation of PLFs, particularly of heavier ones, involves significant overlap of the projectile and the target nuclei. It should be mentioned here that the calculations do not even reproduce the experimental transfer probabilities for channels involving only a few nucleon transfers. This may be due to the fact that even the lowest beam energy in the present study is significantly higher than the entrance channel Coulomb barrier, resulting in a significant nuclear contribution.

For a qualitative comparison of the degree of overlap of the projectile and the target nuclei in the formation of PLFs with $Z_{\rm PLF} = 5$–8, α values are plotted as a function of $E_{\rm c.m.}/V_c$ in Fig. 12. The uncertainty quoted on the α value is due to the fitting error. It can be seen from this figure that α values for all the PLFs systematically decrease with increasing beam energy indicating an increase in nuclear contribution with increasing beam energy. An increase in nuclear contribution with increase in the beam energy suggests that the collision trajectories, involving a significant overlap of the projectile and the target nuclei, start contributing to incomplete fusion reactions at higher beam energies. Such collision trajectories may lead to complete fusion at lower beam energy. Further, at a given beam energy, the α value decreases with increasing mass transfer indicating an increase in nuclear contribution with increasing mass transfer. These observations are consistent with the results of our earlier study in the reaction ^{19}F + ^{89}Y [35]. α values obtained in the reaction ^{19}F + ^{89}Y [35] are also shown in Fig. 12 for comparison. It can be seen from this figure that α values in the reaction ^{19}F + ^{89}Y are systematically higher compared to those in the reaction ^{19}F + ^{66}Zn. This is due to the larger yields of PLFs at forward angles in the reaction ^{19}F + ^{66}Zn compared to that in the reaction ^{19}F + ^{89}Y. The larger yield of PLFs at forward angles in the reaction ^{19}F + ^{66}Zn may be due to the lower entrance

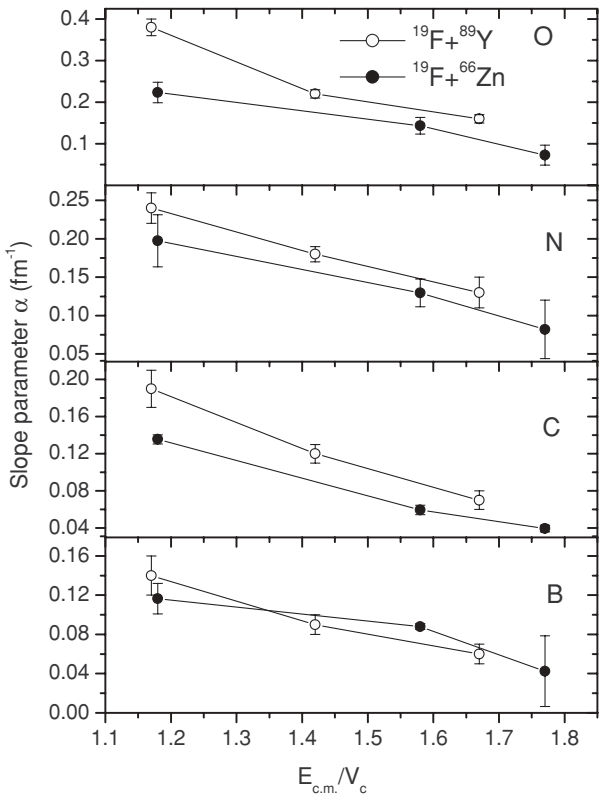

FIG. 12. Plot of slope parameter α for transfer channels involving emission of projectile-like fragments (PLFs) with $Z_{PLF} = 5$–8 in the reactions $^{19}F + {}^{66}Zn$ and $^{19}F + {}^{89}Y$.

channel Coulomb repulsion in the reaction $^{19}F + {}^{66}Zn$ than in the reaction $^{19}F + {}^{89}Y$.

IV. CONCLUSIONS

Cross sections of projectile-like fragments (PLFs) with $Z_{PLF} = 3$–8 have been measured at $E_{lab} = 61, 82, 92$, and 109 MeV. From the angular distributions of PLFs, their formation cross sections were deduced. Experimental cross sections of PLFs were found to be significantly higher compared to those calculated using the sum-rule model, and it was observed that the discrepancy increased with decreasing beam energy. The underestimation of cross sections of PLFs by the sum-rule model is due to the strong preference for complete fusion in this model for collision trajectories with an angular momentum less than limiting angular momentum for complete fusion (l_{lim}(CF)). However, the observation of significant cross sections for incomplete fusion at lower beam energies suggests that incomplete fusion starts competing with complete fusion for $l < l_{lim}$(CF). In order to account for this effect, calculation of the transmission coefficient in the sum-rule model was modified. The modified sum-rule model calculations reproduced the cross sections of PLFs in the present studies.

It has been observed that the cross sections of lighter PLFs decrease more rapidly with decreasing beam energy compared to those of the heavier PLFs. This observation was explained by assuming the formation of lighter PLFs in collision trajectories involving a significant overlap of the projectile and the target nuclei. Transfer probabilities for peripheral collisions were estimated from the nuclear and Coulomb branches of the deflection function. In order to calculate the deflection functions at different beam energies, elastic scattering measurements were carried out to deduce the parameters of nuclear potential. Transfer probabilities calculated assuming peripheral collisions were significantly lower compared to the experimental values, indicating a significant overlap of the projectile and the target nuclei in the formation of PLFs, particularly of lighter PLFs.

Plots of 'experimental transfer probability versus distance of closest approach' were fitted to deduce the slope parameter α for different transfer channels. The α values obtained in the present study were lower compared to those observed in the reaction $^{19}F + {}^{89}Y$ for the respective channels. This may be due to the smaller entrance channel Coulomb repulsion in the reaction $^{19}F + {}^{66}Zn$ compared to that in the reaction $^{19}F + {}^{89}Y$, resulting in a lager yields of PLFs at forward angles in the former reaction. The slope parameter 'α' was observed to decrease with increasing beam energy indicating that the overlap of the projectile and the target nuclei increases with increasing beam energy for a given transfer channel. Further, at a given beam energy, the α value was observed to decrease with increasing mass transfer, indicating an increasing overlap of the projectile and the target nuclei.

ACKNOWLEDGMENT

The authors thank Dr. D. Dutta and Ms. Priya Maheshwari for their help in this experiment.

[1] J. Wilczynski, K. Siwek-Wilczynska, J. Van Driel, S. Gonggrijp, D. C. J. M. Hageman, R. V. F. Janssens, J. Lukasiak, R. H. Siemssen, and S. Y. Van Der Werf, Nucl. Phys. **A373**, 109 (1982).
[2] K. Siwek-Wilczynska, E. H. du Marchie van Voorthuysen, J. van Popta, R. H. Siemssen, and J. Wilczynski, Phys. Rev. Lett. **42**, 1599 (1979).
[3] D. J. Parker, J. J. Hogan, and J. Asher, Phys. Rev. C **35**, 161 (1987).
[4] A. Brondi, M. Kildir, G. La Rana, R. Moro, E. Vardaci, S. Pirrone, F. Porto, S. Sambataro, G. Politi, and P. Figvera, Phys. Rev. C **54**, 1749 (1996).
[5] B. S. Tomar, A. Goswami, G. K. Gubbi, A. V. R. Reddy, S. B. Manohar, Bency John, and S. K. Kataria, Phys. Rev. C **58**, 3478 (1998).
[6] S. Sodaye, K. Sudarshan, B. S. Tomar, A. Goswami, S. Mukherjee, and K. Mahata, Eur. Phys. J. A **14**, 371 (2002).
[7] M. C. Mermaz, Phys. Rev. C **21**, 2356 (1980).
[8] C. K. Gelbke and D. H. Boal, Prog. Part. Nucl. Phys. **19**, 33 (1987).
[9] A. Yokoyama, T. Saito, H. Baba, K. Hata, Y. Nagame, S. Ichikawa, S. Baba, A. Shinohara, and N. Imanishi, Z. Phys. A **332**, 71 (1989).

[10] M. Lunardon *et al.*, Nucl. Phys. **A652**, 3 (1999).
[11] M. C. Mermaz, T. Suomijarvi, R. Lucas, B. Berthier, J. Matuszek, J. P. Coffin, G. Guillaume, B. Heusch, F. Jundt, and F. Rami, Nucl. Phys. **A456**, 186 (1986).
[12] B. G. Harvey, Nucl. Phys. **A444**, 498 (1985).
[13] B. G. Harvey and M. J. Murphy, Phys. Lett. **B130**, 373 (1983).
[14] Adel Y. Abul-Magd, Z. Phys. A **298**, 143 (1980).
[15] M. H. Simbel and A. Y. Abul-Magd, Z. Phys. A **294**, 277 (1980).
[16] T. Udagawa and T. Tamura, Phys. Rev. Lett. **45**, 1311 (1980).
[17] T. Udagawa and T. Tamura, Phys. Lett. **B116**, 311 (1982).
[18] E. Takada, T. Shimoda, N. Takahashi, T. Yamaya, K. Nagatani, T. Udagawa, and T. Tamura, Phys. Rev. C **23**, 772 (1981).
[19] V. I. Zagrebaev, Ann. Phys. (NY) **197**, 33 (1990).
[20] H. Morgenstern, W. Bohne, W. Galster, K. Grabisch, and A. Kyanowski, Phys. Rev. Lett. **52**, 1104 (1984).
[21] H. Morgenstern, W. Bohne, W. Galster, and K. Grabisch, Z. Phys. A **324**, 443 (1986).
[22] E. Gadioli *et al.*, Nucl. Phys. **A708**, 391 (2002).
[23] E. Gadioli *et al.*, Eur. Phys. J. A **17**, 195 (2003).
[24] L. J. Mudau *et al.*, Nucl. Phys. **A761**, 190 (2005).
[25] B. Becker *et al.*, Eur. Phys. J. A **18**, 639 (2003).
[26] E. Z. Buthelezi, F. Cerutti, E. Gadioli, G. F. Steyn, A. Pepe, S. H. Connell, and A. A. Cowley, Eur. Phys. J. A **28**, 193 (2006).
[27] E. Z. Buthelezi, F. Cerutti, E. Gadioli, G. F. Steyna, S. H. Connell, and A. A. Cowley, Nucl. Phys. **A753**, 29 (2005).
[28] M. Cavinato, E. Fabrici, E. Gadioli, Erba E. Gadioli, P. Vergani, M. Crippa, G. Colombo, I. Redaelli, and M. Ripamonti, Phys. Rev. C **52**, 2577 (1995).
[29] C. Birattari *et al.*, Phys. Rev. C **54**, 3051 (1996).
[30] Valery Zagrebaev and Walter Greiner, J. Phys. G **34**, 1 (2007).
[31] Sunita Gupta, B. P. Singh, M. M. Musthafa, H. D. Bhardwaj, and R. Prasad, Phys. Rev. C **61**, 064613 (2000).
[32] Anil Sharma, B. Bindu Kumar, S. Mukherjee, S. Chakrabarty, B. S. Tomar, A. Goswami, and S. B. Manohar, J. Phys. G **25**, 2289 (1999).
[33] M. K. Sharma, Unnati, B. K. Sharma, B. P. Singh, H. D. Bhardwaj, Rakesh Kumar, K. S. Golda, and R. Prasad, Phys. Rev. C **70**, 044606 (2004).
[34] B. Bindu Kumar, Anil Sharma, S. Mukherjee, S. Chakrabarty, P. K. Pujari, B. S. Tomar, A. Goswami, and S. B. Manohar, Phys. Rev. C **59**, 2923 (1999).
[35] R. Tripathi, K. Sudarshan, S. Sodaye, and A. Goswami, J. Phys. G **35**, 025101 (2008).
[36] S. Wald, S. B. Gazes, C. R. Albiston, Y. Chan, B. G. Harvey, M. J. Murphy, I. Tserruya, R. G. Stokstad, P. J. Countryman, K. Van Bibber, and H. Homeyer, Phys. Rev. C **32**, 894 (1985).
[37] C. Gerschel, Nucl. Phys. **A387**, 297c (1982).
[38] T. Inamura, A. C. Kahler, D. R. Zolnowski, U. Garg, T. T. Sugihara, and M. Wakai, Phys. Rev. C **32**, 1539 (1985).
[39] K. Sudarshan, S. Sodaye, K. Surendra Babu, S. Mukherjee, S. K. Rathi, K. Mahata, A. Goswami, and B. S. Tomar, Phys. Rev. C **69**, 027603 (2004).
[40] B. S. Tomar, K. Surendra Babu, K. Sudarshan, R. Tripathi, and A. Goswami, Pramana J. Phys. **64**, 221 (2005).
[41] R. Bass, *Nuclear Reactions with Heavy Ions* (Springer-Verlag, Berlin, 1980).
[42] K. E. Rehm, B. G. Glagola, W. Kutschera, F. L. H. Wolfs, and A. H. Wuosmaa, Phys. Rev. C **47**, 2731 (1993).
[43] B. K. Nayak, R. K. Choudhury, D. C. Biswas, L. M. Pant, A. Saxena, D. M. Nadkarni, and S. S. Kapoor, Phys. Rev. C **55**, 2951 (1997).
[44] D. C. Biswas, R. K. Choudhury, B. K. Nayak, and D. M. Nadkarni, Phys. Rev. C **56**, 1926 (1997).
[45] P. K. Sahu, R. K. Choudhury, D. C. Biswas, and B. K. Nayak, Phys. Rev. C **64**, 014609 (2001).
[46] J. P. Bondorf, F. Dickmann, D. H. E. Gross, and P. J. Siemens, J. Phys. Colloque. **32**, C6-145 (1971).
[47] J. Wilczynski, Nucl. Phys. **A216**, 386 (1973).
[48] L. Corradi *et al.*, Z. Phys. A **335**, 55 (1990).
[49] P. R. Christensen, V. I. Manko, F. D. Becchetti, and R. J. Nickles, Nucl. Phys. **A207**, 33 (1973).
[50] P. Schwandt, optical model code SNOOPY 8Q , Indiana University, 1984.